AIP | Journal of Applied Physics

Development and experimental characterization of a wall-less Hall thruster

S. Mazouffre, S. Tsikata, and J. Vaudolon

Citation: Journal of Applied Physics **116**, 243302 (2014); doi: 10.1063/1.4904965
View online: http://dx.doi.org/10.1063/1.4904965
View Table of Contents: http://scitation.aip.org/content/aip/journal/jap/116/24?ver=pdfcov
Published by the AIP Publishing

Development and experimental characterization of a wall-less Hall thruster

S. Mazouffre,[a] S. Tsikata, and J. Vaudolon
ICARE, CNRS, 1C avenue de la Recherche Scientifique, 45071 Orléans, France

(Received 8 October 2014; accepted 11 December 2014; published online 23 December 2014)

An alternative Hall thruster architecture that shifts the ionization and acceleration regions outside the plasma chamber is demonstrated. This unconventional design is here termed a "wall-less Hall thruster," as the bulk of the magnetized discharge is no longer limited by solid boundaries. A 200 W prototype with permanent magnets has been developed and characterized. Experimental results concerning the thruster operation, discharge oscillations, electric field distribution, and ionization zone characteristics are presented and discussed. Our first experiments show that the cross-field discharge can be moved outside the cavity without drastically disturbing the ion production and acceleration mechanisms. This design offers the benefit of reduced plasma-wall interaction and lower wall losses, while also greatly facilitating diagnostic access to the entire discharge ionization and acceleration regions. © *2014 AIP Publishing LLC*. [http://dx.doi.org/10.1063/1.4904965]

I. INTRODUCTION

The change from chemical to electrical propulsion systems for satellites and spacecraft allows a drastic reduction in the propellant mass, as a direct consequence of the higher propellant ejection speed. This aspect of spaceflight is illustrated through the Tsiolkovsky rocket equation.[1,2] The mass reduction can translate into various benefits, according to the mission profile and objective: cost-savings, reduction of launch vehicle class, increase in satellite payload mass, and extension of probe capacity in the case of deep-space travel.

Many different types of electrical thrusters exist, usually classified according to their thrust level and their operating principle, i.e., thermal, electrostatic, or electromagnetic.[3–5] The Hall Thruster (HT) is one of the most advanced and mature technologies with a flight heritage dating to 1971. Hall thrusters deliver a moderate propellant ejection speed compared to gridded ion sources; however, they furnish a large thrust-to-power ratio. They are therefore well-suited for more rapid maneuvers. They are currently used for station-keeping and attitude control of geosynchronous communication satellites. Orbit raising has recently been achieved with the AEHF satellite. In the very near future, high-power Hall thrusters will also permit maneuvers with a large velocity increment such as orbit transfer, rendering all-electric satellites a reality. In addition, as proven by the successful SMART-1 lunar mission, HTs are good candidates for solar system exploration.

Hall thrusters are efficient gridless ion accelerators.[6–8] Their operating principle relies on the creation of a low-pressure, quasi-neutral plasma discharge in crossed magnetic and electric fields. In the standard configuration, the magnetized DC discharge is confined to an annular dielectric cavity with the anode at one end, where the gas is injected, and an external cathode that also serves as beam neutralizer. Xenon is typically used as the propellant gas for its specific properties of high atomic mass and low ionization energy. A set of solenoids or permanent magnets provides a radially directed magnetic field, the strength of which is maximum at the channel exhaust. The magnetic field is chosen strong enough to make the electron Larmor radius much smaller than the mean free path between electron collisions, but weak enough not to affect ion trajectories. The electric potential drop is mostly concentrated in the final section of the channel owing to the high electron resistivity there. The corresponding axial electric field drives a large azimuthal electron drift—the Hall current—which is responsible for the efficient ionization of the gas. The electric field also accelerates ions, generating thrust. A schematic cross-section view of a conventional Hall thruster is shown in Fig. 1.

The architecture and working principle of a Hall thruster offer several advantages: a high efficiency, simple, compact, and robust design as well as a large thrust level. The main drawback of conventional HTs is the relatively short operational lifetime, especially when compared to gridded ion engines. This weakness has its origin in plasma-surface interaction inside the discharge chamber. Plasma-surface interaction is a very general problem in plasma physics that applies to many plasma source technologies.[9–11] The primary

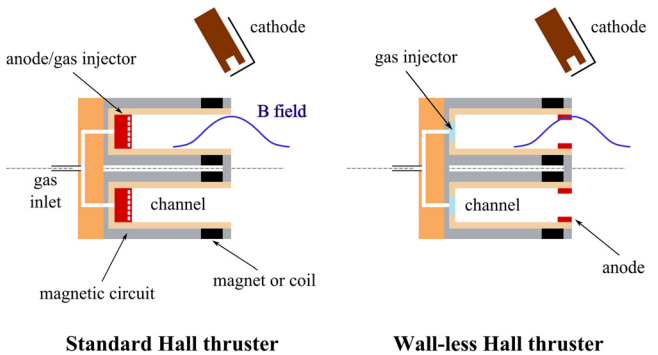

FIG. 1. (Left) Layout of the configuration of a standard single-stage Hall thruster. The anode is placed at the back of an annular ceramic channel. The magnetic field is maximum at the channel exit plane. (Right) Basic transformation into a wall-less HT. The anode is shifted towards the channel exit plane. The other elements remain unchanged.

[a]Author to whom correspondence should be addressed. Electronic mail: stephane.mazouffre@cnrs-orleans.fr

limiting factor for the lifetime is the erosion of the annular channel walls due to bombardment by hot electrons and high-energy ions.[12,13] The wall material affects, to a large extent, the plasma discharge properties and dynamics, and consequently, the performance level and the lifetime of the device. In the case of a HT, the wall dielectric material influences the plasma properties mainly through secondary electron emission,[14–18] which has three main consequences. First, the bulk electron temperature decreases because of the injection of cold electrons and loss of hot electrons to the walls. Second, the transverse electron transport across the magnetic field is enhanced.[19] Finally, the sheath strength diminishes due to space charge saturation, causing the potential drop that usually repels electrons to reduce and a large particle flux to reach the wall.

One means of reducing the effect of plasma-surface interaction in a Hall thruster is to modify the channel geometry in order to decrease the surface-to-volume ratio. In a low-pressure discharge, the plasma is produced in the volume while losses occur at the walls. Increasing the channel width of a HT, while maintaining the mean diameter, has been proven in a previous study to reduce the power losses and increase the ionization and the thrust efficiency.[20] This study, however, did not provide evidence of a positive impact on the thruster lifetime as no endurance testing was performed.

Another means of decreasing plasma-surface interaction consists of altering the magnetic field topology. As previously explained, in a HT, the accelerating electric field is provided by a decrease of the electron mobility in the vicinity of the channel exhaust where the magnetic field magnitude is large. However, an efficient magnetic barrier requires a radial magnetic field, the lines of which intersect the walls, resulting in particle transport to the walls.

Recently, an original approach to significantly reducing the charged-particle flux to the channel walls, hence prolonging the thruster lifetime, has been proposed and validated. This approach is termed magnetic shielding (MS).[21–26] MS consists of preventing the magnetic field lines from crossing the walls in the acceleration region. The MS field topology is formed by these parallel lines near the walls, also termed "grazing lines," which extend to the anode region where electrons are cold. This in turn allows the maintenance of a high plasma potential in front of the walls. Such a topology strongly reduces the magnitude of the radial electric field component, thereby decreasing ion energy and the wall material erosion rate without decreasing the performance.

There is another more drastic alternative to limiting the interaction between plasma and surfaces in a HT. The principle is to entirely shift the ionization and acceleration regions outside the cavity. This unconventional design is named here a Wall-Less Hall Thruster, or WL-HT in short. Such an unusual configuration was in fact first explored during the 90s in Russia by Kapulkin *et al.*[27,28] At that time, the concept was introduced as a Hall thruster with an external electric field. However, due to a presumed ion current limitation linked to plasma instabilities, researchers moved from a standard one-stage architecture to a two-stage architecture. The design and operation of the latter are more complicated, making the concept somewhat less attractive. The possibility of shifting the electric field outside the device was also studied in Russia at TsNIIMASH with single-stage thrusters with anode layer (TAL) in the late 90s and early 2000s.[29] With this configuration, they demonstrated possible stable operation at high discharge voltage with a high efficiency. To the best of our knowledge, research into the external electric field concept was abandoned. In this article, we revisit the concept of single-stage Hall thrusters with an external plasma discharge through the building, testing and preliminary characterization of a low-power, permanent-magnet, wall-less Hall thruster prototype.

II. WALL-LESS HALL THRUSTER PROTOTYPE

The standard configuration of a Hall thruster is schematically depicted in Fig. 1. Additional details can be found elsewhere.[6–8] The anode is placed at the back of an annular ceramic channel. In many designs, the anode is also used as a gas injector. The cathode, which produces the electron current for discharge balance and ion beam neutralization, is located outside the channel. To shift both the ionization and the acceleration regions outside the thruster cavity, the simplest way is to move the anode towards the channel exit plane, as illustrated in Fig. 1, without other modifications. The thruster shape and size remain unchanged, as do the cavity material and the magnetic field topology. This is the basic method for transforming a HT into a WL-HT; however, optimization of the thruster in its new configuration will certainly require other changes. When moving the anode to the exit, one of two conditions must be fulfilled to minimize ion losses inside the channel. The potential drop inside the channel, if any, must be small and/or the ion fraction inside the channel must be low. Another point must be addressed here. A Wall-Less Hall thruster is not a TAL, as there is no guard ring at the cathode potential in front of the anode to localize the potential drop.[7,30] In a WL-HT, the distribution of the plasma potential downstream the exit plane is solely fixed by a balance between ionization and diffusion processes in a magnetized plasma.

A photograph of the WL-HT prototype constructed in our laboratory is shown in Fig. 2. The prototype is based on the architecture of a 200 W-class Hall thruster, which

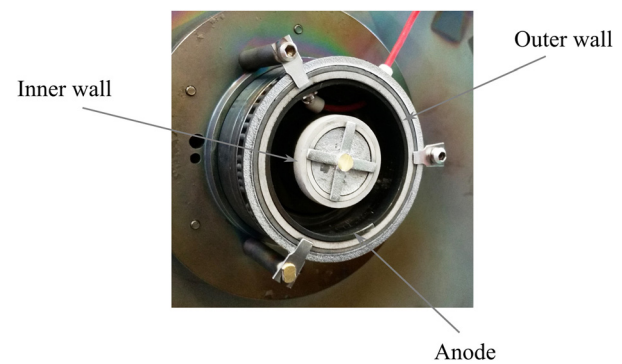

FIG. 2. Photograph of the 200 W-class WL-HT prototype. The anode is a conducting ring located at the channel exit plane around the external wall. The cavity walls are made of BN-SiO_2. The magnetic field is generated with permanent magnets.

delivers a thrust of 10 mN when operated at 250 V and 1.0 mg/s xenon mass flow rate.[20,31] This thruster exhibits four interesting features that make it highly versatile. First, the magnetic field is generated via small samarium–cobalt (SmCo) magnets brought together inside rings located on either side of the channel walls. A soft iron magnetic circuit with a back gap permits the channeling of the magnetic flux such that the desired topology is obtained. No magnetic screen is used. The magnetic field strength can easily be modified by a variation of the number of magnets. Second, the propellant gas is injected homogeneously inside the channel using a porous ceramic located at the back of the channel. In the standard configuration, a stainless-steel ring placed at the back of the channel serves as anode. Third, a central copper heat sink is employed to evacuate heat towards a radiator placed behind the thruster. Finally, the width of the channel can easily be modified while the mean diameter remains unchanged, by means of various sets of ceramic rings.

In this study, the channel dielectric walls of the WL-HT were made of BN-SiO_2. The channel was in the $2S_0$ configuration, meaning that the width-to-mean diameter ratio was twice the standard ratio,[20] where this standard ratio is defined as that of the well-known Russian SPT100 thruster. As demonstrated in a preceding study, a broad channel improves the performance level of a Hall thruster in terms of thrust, mass utilization, ion production cost, ion velocity, thermal load, and operation envelope.[20] The anode used for the wall-less prototype is a 5 mm-wide stainless steel ring. It is wound around the external wall at the channel exit plane, where the magnetic field amplitude is the highest. Xenon is used as a propellant gas. A heated hollow cathode with a LaB_6 insert was used with a constant mass flow rate of 0.2 mg/s. The cathode orifice was placed 10 cm below the thruster symmetry axis in radial direction and 3 cm away from the channel exit plane in axial direction. The cathode and the thruster body are floating but unbound.

III. DISCHARGE AND BEAM PROPERTIES

A. Source operation

All experiments have been performed in the NExET (New Experiments on Electric Thrusters) vacuum chamber. The test-bench is a stainless steel vacuum vessel 1.8 m in length and 0.8 m in diameter. It is equipped with a pump stack composed of a large dry pump, a 350 l/s turbomolecular pump to evacuate light gases, and a cryogenic pump with a typical surface temperature of 35 K to remove gases such as xenon and krypton. A large water-cooled screen covered with graphite tiles is mounted at the back of the chamber. The screen absorbs a part of the ion beam energy, thereby reducing the thermal load on the cryogenic surface. A background pressure of 3×10^{-5} mbar-Xe (2.2×10^{-5} Torr-Xe) is achieved with 1.2 mg/s xenon gas flow rate and 400 W input power. Under identical conditions, the pressure is typically 10^{-4} mbar-Kr with krypton gas. The heavy particle momentum exchange mean free path is, in this backpressure condition, on the order of the chamber length, which guarantees a negligible impact of the residual gas.

Figure 3 shows a set of photographs of the low-power ion source firing with Xe in the NExET vacuum chamber in the standard configuration and in the wall-less configuration with a ring anode. Pictures were taken with the same camera settings. The operating conditions were a discharge voltage U_d of 200 V and a gas mass flow rate of 1 mg/s. The background gas pressure inside the tank was 3.5×10^{-5} mbar-Xe.

The photos show that the plasma discharge is moved outside the dielectric cavity in the wall-less configuration, as illustrated by the strong light intensity in front of the exit plane. It is also interesting to note that the ion beam boundaries are less sharp in the WL configuration. For instance, the brightness of the on-axis, collimated structure that originates from the interaction of elementary beams from opposite sides of the channel, seen in the photographs on the left, is fainter in the WL configuration, which certainly images

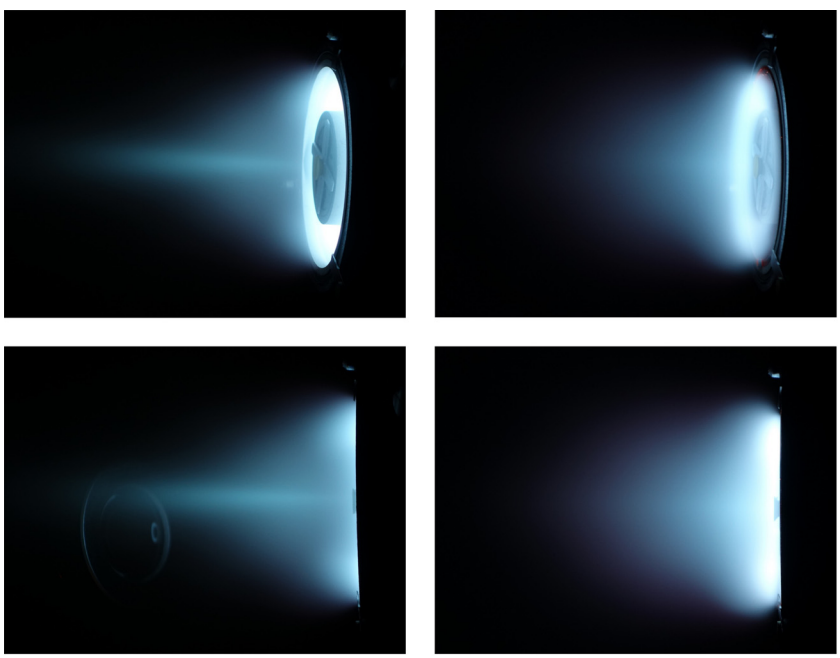

FIG. 3. (Left) Photographs of the low-power Hall thruster firing with Xe at 200 V and 1 mg/s in standard configuration. (Right) Photographs of the WL-HT prototype firing with Xe under identical conditions. In the latter case, the anode is a conducting ring located at the channel exit plane around the external wall.

deteriorated performances. According to the photos, the WL configuration is expected to lead to a larger ion beam divergence angle. As a consequence, the thrust will be lower and the wear of the external parts like the pole pieces could be increased. In addition, a large beam divergence can have a negative impact on the interaction between the plasma and the spacecraft elements.

B. Current-voltage characteristics

The discharge current waveforms measured on the anode line at 200 V and 260 V and 1 mg/s are presented in Fig. 4 for the two thruster configurations. The current was measured with a calibrated Tektronix TCP202 DC coupled current-probe (DC to 50 MHz bandwidth). The mean value of I_d is always larger in the WL-HT. At 200 V and 260 V, it is, respectively, 1.05 A and 1.14 A for the WL-HT. At 200 V and 260 V, the current is, respectively, 0.89 A and 0.90 A in the standard thruster. On the contrary, the standard deviation of the discharge current is lower is wall-less mode. At 200 V and 260 V, it is, respectively, 0.16 A and 0.15 A for the WL-HT. At 200 V and 260 V, the dispersion is, respectively, 0.17 A and 0.24 A in the standard thruster. As in a conventional Hall thruster, the current trace of a thruster with an external discharge exhibits low-frequency oscillations in the 10–30 kHz range that correspond to the well-known breathing mode.[32] Such oscillations, which find their origin in an ionization instability, can be interpreted in terms of a predator-prey type of mechanism between atoms and ions.[33,34] Also shown in Fig. 4 are the power spectra associated with the discharge current time series. The power spectra were computed using a FFT algorithm. In Figure 4, the breathing oscillation frequency is between 20 kHz and 25 kHz. The breathing frequency is not influenced by the thruster design, an indication that the main physical processes that govern ionization in the cross-field discharge remain unchanged. The power spectrum also shows strong oscillations around 100 kHz in the standard configuration. These oscillations encompass phenomena such as rotating instabilities and ion transit time instabilities.[32] These oscillatory phenomena are absent, or at least much weaker, in WL-HT whatever the operating conditions.

The graph in Fig. 5 shows the anode discharge current as a function of the applied voltage for various xenon gas mass flow rates. The current-mass flow rate envelope is similar for the two configurations, i.e., the thruster can operate with the same parameters. However, the discharge current is higher in the case of the WL-HT whatever the voltage-flow rate couple. The difference increases with the gas flow rate and the applied voltage. Moreover, the rate of change of I_d with U_d is positive in WL, whereas it is negative in standard mode for most flow rates. As the maximum input power is allowed to exceed 300 W only for a short time to prevent damage to the device, the WL mode is limited in voltage at large mass flow rate. The origin of the difference in discharge current remains to be understood. An increase in the propellant utilization is unlikely as the ionization efficiency of the thruster with a conventional design is already high.[20] As can be seen in Fig. 5, at 200 V, the current increases from 1.34 A to 2.21 A when the configuration is switched from a standard to a WL-HT mode (an increase of 64%). Such an increase cannot be attributed solely to improved gas ionization. The large discharge current in the WL mode is more likely due to a larger diffusion of the electrons in the region of strong magnetic field. With the present non-optimized WL-HT thruster design, the electron mobility is enhanced in front of the thruster. Many magnetic field lines, especially the ones that extend far downstream, intersect the anode, making the passage of electrons to the anode easier. A larger radial ion current and a higher amount of multiply charged ion species are also expected.

Figure 5 also shows that the discharge current standard deviation is not greatly affected when the anode is moved towards the channel exit plane. That confirms the oscillation level of the breathing mode does not depend on the configuration, see Fig. 4. This fact reveals that, overall, the ionization and acceleration mechanisms do not change, or, in other

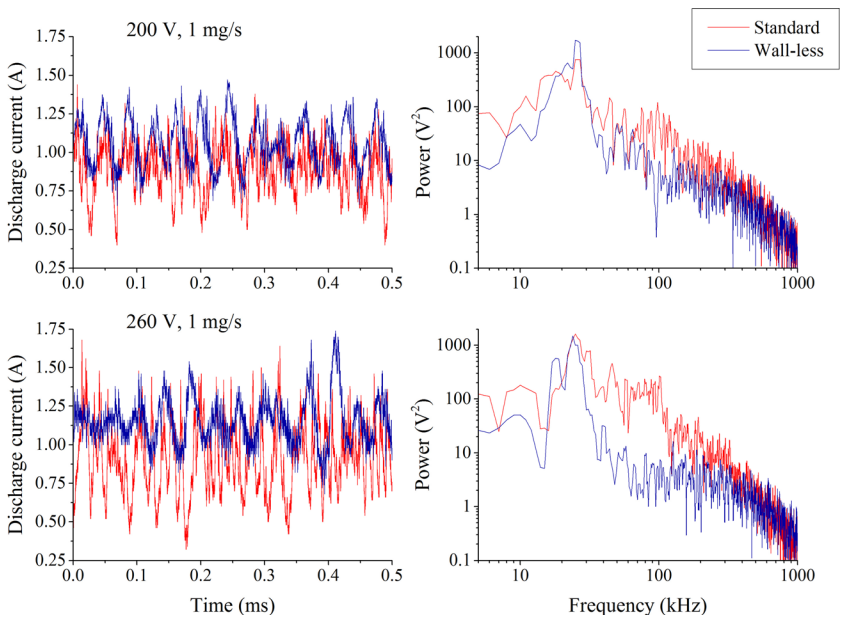

FIG. 4. (Left) Discharge current waveforms of the thruster in the standard configuration and in the wall-less configuration for two different applied voltages. (Right) Corresponding power spectra computed using a FFT algorithm.

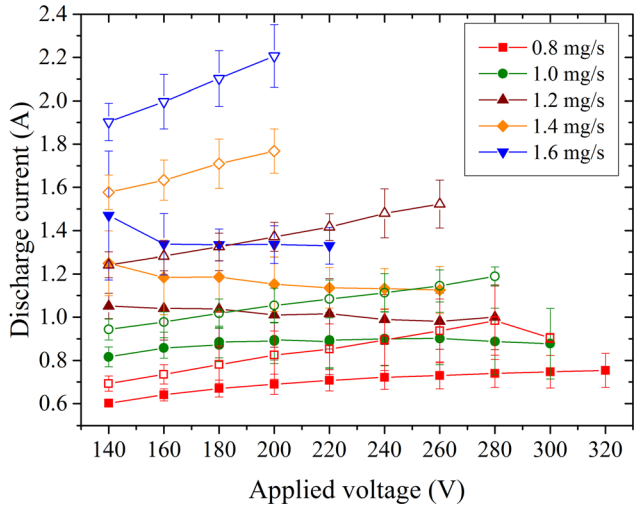

FIG. 5. Anode discharge current against applied discharge voltage for several xenon mass flow rates in the standard (full symbols) and WL-HT configurations (open symbols). Error bars indicate the current standard deviation.

words, the underlying physics remains unchanged at the macroscopic level.

C. Ion velocity and electric field distribution

The time-averaged distribution function of the axial velocity component of metastable Xe^+ ions was measured along the channel axis of the Hall thruster by means of laser induced fluorescence spectroscopy at 834.72 nm for the two configurations. Details of the experimental arrangement and the LIF technique and optical bench can be found elsewhere.[31,35] In Figure 6, the most probable ion velocity, i.e., the velocity for which the VDF is the highest, is plotted as a function of the position x along the channel axis for a discharge voltage of 200 V and a gas flow rate of 1 mg/s. The position $x = 0$ refers to the channel exit plane. With a standard design, the ion acceleration process starts upstream of the exit plane. At $x = 0$ mm, the ion velocity is already 5200 m/s. Beyond the exit plane, the velocity increases over a short distance of about 20 mm and attains a maximum ion velocity of 15 200 m/s. With the wall-less prototype, the acceleration region is entirely shifted outside the channel. The velocity is typically 150 m/s inside the channel. This value is close to the thermal speed for xenon atoms at 300 K. The maximum velocity is 13 510 m/s. It is worth noting that the atom velocity is typically 500 m/s at the channel exhaust in the standard configuration.[35,36] This large atom velocity, well above the thermal speed, can only be explained by taking into account ion recombination at the walls to form fast neutrals.[36] The very low ion axial velocity inside the cavity of a WL-HT source is therefore an indirect proof that plasma-surface interaction has been strongly reduced.

The accelerating potential, also called the beam energy V_b, corresponds to the potential drop experienced by the ions. It is directly computed from the velocity. In the standard configuration, V_b is 160 eV, whereas it is only 120 eV in the WL-HT. The low final ion axial velocity, i.e., the low beam energy, in WL configuration indicates a poor energy conversion efficiency in the axial direction. Energy losses may originate in the strong curvature of the magnetic field lines in the acceleration region, which makes the ion beam diverge, as suggested by Fig. 3. The low beam energy indicates that the WL configuration must be improved and optimized. Possible ways are discussed in the concluding section.

In steady-state conditions, the accelerating electric field profile can be directly inferred from the profile of the ion velocity axial component using the energy conservation equation.[35,37] The electric field distribution along the channel axis of the WL-HT is shown in Fig. 7 for 200 V and 1 mg/s. The electric field profile measured in the conventional configuration is also shown in Fig. 7 for comparison. As expected, the electric field is situated outside the cavity in the WL-HT. The length of the acceleration region is about 15 mm, similar to the size observed with the standard configuration. The shift of the electric field towards the exterior has been observed for other experimental parameters: 150 V and 0.8 mg/s and 85 V and 1.3 mg/s.[38] The wall-less condition is only driven by the anode position, but the electric field shape depends on the operating parameters.

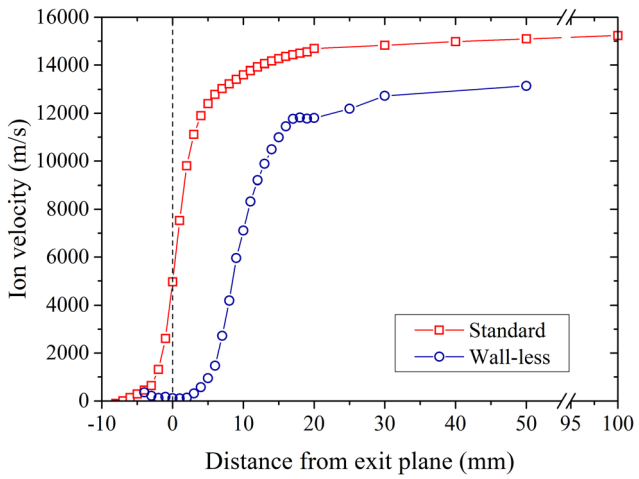

FIG. 6. Most probable Xe^+ ion velocity along the channel axis of the ion source in standard (square) and WL-HT (circle) configurations (200 V, 1 mg/s).

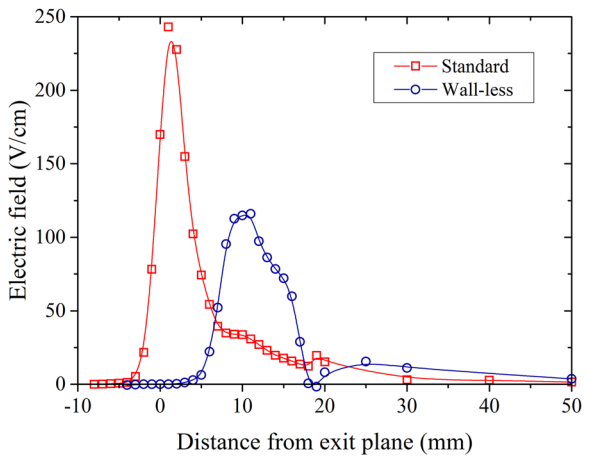

FIG. 7. Accelerating electric field distribution along the channel axis of the ion source in the standard (square) and WL-HT (circle) configurations (200 V, 1 mg/s).

In summary, in the wall-less mode the electric field exists in a region (i) with no physical boundary in the radial direction and (ii) where the magnetic field gradient is negative. LIF measurements demonstrate that the interaction between high energy ions and ceramic surfaces is negligible in a Hall thruster with a shifted anode. This aspect is obviously of great relevance for allowing high-voltage operation and for prolonging the lifetime of the device.

D. Ionization

A direct measurement of the spatial extent of the ionization region, e.g., by means of a Langmuir probe, is not yet available. We have, however, indirect evidence that a large fraction of ions are produced outside the channel. Figure 8 shows three normalized Xe^+ ion VDF measured by near-infrared LIF along the channel centerline of the WL-HT at 85 V and 1.3 mg/s. The width, or dispersion, of the VDF is observed to change with axial position. The VDF is relatively narrow at the exit plane as well as far downstream. In contrast, the VDF is very broad a few millimeters behind the exhaust. In a Hall thruster discharge, the ion velocity dispersion is mostly determined by the overlap between the ionization region and the acceleration region.[35] Moreover, the largest dispersion indicates the end of the ionization region.[35,39] With a standard design, the ionization layer ends at the exit plane. The shape of the ion VDF in Fig. 8 shows that a large part of the ionization process occurs outside the channel of the wall-less Hall thruster, as the highest dispersion is reached beyond $x = 10$ mm.

E. Erosion and thermal state

Visual observation of the thruster prototype firing and measurements of various quantities indicate that a non-optimized WL configuration leads to a high plume divergence angle and to a large discharge current, with possible consequences for the erosion level and thruster heating. There was no visible sign of accelerated erosion of pole pieces or other elements after several tens of hours of operation. In like manner, we did not observe deposit formation inside the ceramic channel. However, more precise erosion measurements and longer-term endurance testing will be necessary to confirm these preliminary observations.

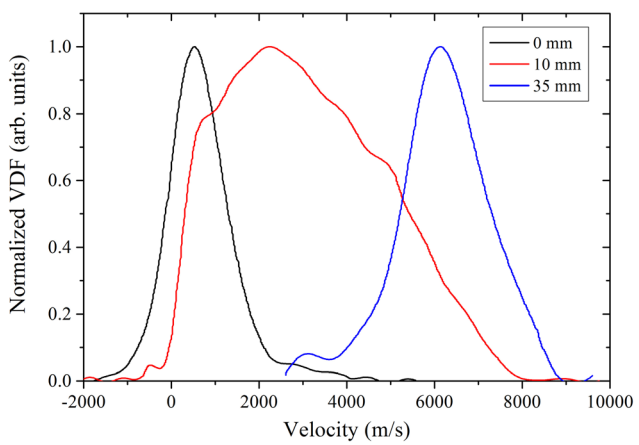

FIG. 8. Xe^+ ion VDF at 3 positions along the channel axis of the wall-less HT (85 V, 1.3 mg/s). The position $x = 0$ refers to the exit plane.

The temperature of the WL-HT components was not recorded during the campaign. However, at large gas mass flow rate, i.e., when the discharge current is large (Fig. 5), a hotspot appeared on the anode ring and the thruster could only be operated for a few minutes, indirect evidence that the thermal load of a WL-HT is large compared to a standard configuration. Despite the shifting of the acceleration region beyond the exit plane, the particle flux to the walls at the location of the anode is considerable. Optimization of the magnetic field topology should limit this flux.

IV. CONCLUSIONS

An alternative Hall thruster architecture that shifts the ionization and acceleration regions outside the cavity has been developed, tested, and characterized in part. The objectives of this work were multiple: (i) to verify the possibility of moving the ionization zone and the electric field entirely outside the cavity, while still ensuring thruster operation, (ii) to evaluate the potential of the design with benefits and drawbacks, and (iii) to propose an optimization strategy. First experimental results using this design, concerning thruster operation, discharge oscillations, electric field distribution, and the ionization zone indicate that (i) the magnetized discharge can be moved outside the cavity without significantly compromising the ion production and acceleration and (ii) the discharge is stable although magnetic field gradients are negative. This study also reveals deterioration of the performances as well as drawbacks in the wall-less configuration: The beam energy is low, the divergence is large, the discharge current is high, and the interaction of the plasma with the thruster poles and covers is probably increased. Further optimization of several parameters will therefore be necessary to recover a high efficiency.

A high-efficiency Hall thruster in the WL configuration with an external electric field would offer significant benefits for spacecraft propulsion in terms of integration, operating envelope, lifetime, and fuel options. As the thrust is generated outside, the dielectric channel can be considerably shortened, leading to economies in mass and volume. Plasma interaction with the walls will have been significantly reduced. The cavity material will therefore have less influence on the thruster performance, and more importantly, operation at high voltage is presumably possible and lifetime can be extended. Furthermore, reduction in plasma-wall interactions could lead to the achievement of larger electron temperature, a positive point for efficient ionization of atomic fuels like krypton and argon. On the other hand, plume-spacecraft interaction might represent a critical issue if the plume divergence angle stays large for a WL-HT.

The optimization of a Hall thruster in the WL configuration will require measurements of electron properties, ion current, ion velocity, and thrust. Given the outcomes of this recent investigation, the optimization strategy will be focused on different aspects. The magnetic field strength and topology must be changed; the field magnitude can be increased to enhance trapping of the electrons, and the

magnetic flux inside the cavity minimized. A low magnetic field line curvature in the acceleration region would be preferable for reducing the radial electric field component and the beam divergence. Intersection between the anode and the flux lines is to be avoided in order to prevent short-circuiting of the magnetic barrier. The anode geometry must also be modified to make the system more symmetrical. The width of the anode must also be reduced to limit the plasma diffusion inside the cavity. A high-transparency grid located at the anode plane could be a good option, as suggested by recent experiments.[38] Finally, the length of the ceramic cavity must be decreased, while remaining long enough to guarantee homogenization of the injected gas. Shortening the source will have the benefit of decreasing its mass and volume.

A wall-less ion source provides an ideal platform for the study of cross-field discharge configurations with sophisticated tools like Thomson scattering (coherent and incoherent) and LIF spectroscopy. The access it provides to key regions in the plasma facilitates a thorough investigation of plasma instabilities, discharge oscillations, and small-scale turbulence for a better understanding of the discharge physics, anomalous electron transport and the influence of secondary electron emission. The wall-less source also represents a good test-case for physical modelling and associated numerical simulations of the discharge due to the greatly simplified boundary conditions.

ACKNOWLEDGMENTS

J. Vaudolon benefits from a CNES/Snecma PhD grant.

[1]M. J. L. Turner, *Rocket and Spacecraft Propulsion* (Springer-Praxis Publishing Ltd, Chichester, UK, 2009).
[2]R. H. Frisbee, "Advanced space propulsion for the 21st century," J. Propul. Power **19**, 1129 (2003).
[3]E. Ahedo, "Plasma for space propulsion," Plasma Phys. Controlled Fusion **53**, 124037 (2011).
[4]M. Martínez-Sánchez and J. E. Pollard, "Spacecraft electric propulsion: An overview," J. Propul. Power **14**, 688 (1998).
[5]L. Garrigues and P. Coche, "Electric propulsion: Comparison between different concepts," Plasma Phys. Controlled Fusion **53**, 124011 (2011).
[6]D. M. Goebel and I. Katz, *Fundamentals of Electric Propulsion* (Wiley, Hoboken, 2008), pp. 385-392.
[7]V. V. Zhurin, H. R. Kaufmann, and R. S. Robinson, "Physics of closed drift thrusters," Plasma Sources Sci. Technol. **8**, R1 (1999).
[8]K. Dannenmayer and S. Mazouffre, "Elementary scaling relations for Hall effect thrusters," J. Propul. Power **27**, 236 (2011).
[9]J. P. Chang and J. W. Coburn, "Plasma-surface interactions," J. Vac. Sci. Technol. A **21**, S145 (2003).
[10]A. W. Kleyn, W. Koppers, and N. Lopes Cardozo, "Plasma-surface interaction in ITER," Vacuum **80**, 1098 (2006).
[11]N. Gascon, M. Dudeck, and S. Barral, "Wall material effects in stationary plasma thrusters. I. Parametric studies of a SPT-100," Phys. Plasmas **10**, 4123 (2003).
[12]S. Mazouffre, J. Pérez Luna, and K. Dannenmayer, "Examination of plasma-wall interactions in Hall effect thrusters by means of calibrated thermal imaging," J. Appl. Phys. **102**, 023304 (2007).
[13]S. Mazouffre, K. Dannenmayer, and C. Blank, "Impact of discharge voltage on wall-losses in a Hall thruster," Phys. Plasmas **18**, 064501 (2011).
[14]S. Barral, K. Makowski, Z. Peradzyński, N. Gascon, and M. Dudeck, "Wall material effects in stationary plasma thrusters. II. Near-wall and in-wall conductivity," Phys. Plasmas **10**, 4137 (2003).
[15]Y. Raitses, D. Staack, and N. J. Fisch, "Electron-wall interaction in Hall thrusters," Phys. Plasmas **12**, 057104 (2005).
[16]Y. Raitses, A. Smirnov, D. Staack, and N. J. Fisch, "Measurements of secondary electron emission effects in the Hall thruster discharge," Phys. Plasmas **13**, 014502 (2006).
[17]E. Ahedo, J. M. Gallardo, and M. Martínez-Sánchez, "Effects of the radial plasma-wall interaction on the Hall thruster discharge," Phys. Plasmas **10**, 3397 (2003).
[18]E. Ahedo and V. De Pablo, "Combined effects of electron partial thermalization and secondary emission in Hall thruster discharges," Phys. Plasmas **14**, 083501 (2007).
[19]I. D. Kaganovich, Y. Raitses, D. Sydorenko, and A. Smolyakov, "Kinetic effects in a Hall thruster discharge," Phys. Plasmas **14**, 057104 (2007).
[20]S. Mazouffre, G. Bourgeois, K. Dannenmayer, and A. Lejeune, "Ionization and acceleration processes in a small, variable channel width, permanent-magnet Hall thruster," J. Phys. D: Appl. Phys. **45**, 185203 (2012).
[21]I. G. Mikellides, I. Katz, R. R. Hofer, D. M. Goebel, and K. deGrys, "Magnetic shielding of the channel walls in a Hall plasma accelerator," Phys. Plasmas **18**, 033501 (2011).
[22]I. G. Mikellides, I. Katz, R. R. Hofer, and D. M. Goebel, "Magnetic shielding of walls from the unmagnetized ion beam in a Hall thruster," Appl. Phys. Lett. **102**, 023509 (2013).
[23]I. G. Mikellides, I. Katz, R. R. Hofer, and D. M. Goebel, "Magnetic shielding of a laboratory Hall thruster. I. Theory and validation," J. Appl. Phys. **115**, 043303 (2014).
[24]R. R. Hofer, D. M. Goebel, I. G. Mikellides, and I. Katz, "Magnetic shielding of a laboratory Hall thruster. II. Experiments," J. Appl. Phys. **115**, 043304 (2014).
[25]D. M. Goebel, R. R. Hofer, I. G. Mikellides, I. Katz, J. E. Polk, and B. Dotson, "Conducting wall Hall thrusters," in *Proceedings of 33rd International Electric Propulsion Conference* (Washington DC), IEPC Paper 13–276 (2013).
[26]S. Mazouffre, J. Vaudolon, G. Largeau, C. Hénaux, A. Rossi, and D. Harribey, "Visual evidence of magnetic shielding with the PPS-Flex Hall thruster," IEEE Trans. Plasma Sci. **42**, 2668 (2014).
[27]A. M. Kapulkin, A. D. Grishkevich, and V. F. Prisnyakov, "Outside electric field thruster," in *Proceedings 45th IAF Congress; Space Technol.* (Pergamon, UK), Vol. 15, pp. 391–394 (1995).
[28]V. F. Prisnyakov, A. N. Petrenko, A. M. Kapulkin, I. N. Statsenko, A. I. Kondratiev, and S. N. Kulagin, "The review of the works on electrical propulsion thrusters development and investigation carried out at the Dnepropetrovsk State University," in *Proceedings 24th International Electric Propulsion Conference* (Moscow, Rusia), IEPC Paper 95–12 (1995).
[29]A. Semenkin, "External anode layer thruster parameters at a high specific impulse regimes," in *Proceedings 25th International Electric Propulsion Conference* (Cleveland, Ohio), IEPC paper 97–055 (1997).
[30]M. Keidar, Y. Choi, and I. D. Boyd, "Modeling a two-stage high-power anode layer thruster and its plume," J. Propul. Power **23**, 500 (2007).
[31]A. Lejeune, G. Bourgeois, and S. Mazouffre, "Kr II and Xe II axial velocity distribution functions in a cross-field ion source," Phys. Plasmas **19**, 073501 (2012).
[32]E. Y. Choueri, "Plasma oscillations in Hall thrusters," Phys. Plasmas **8**, 1411 (2001).
[33]S. Barral and E. Ahedo, "Low-frequency model of breathing oscillations in Hall discharges," Phys. Rev. E **79**, 046401 (2009).
[34]J. P. Boeuf and L. Garrigues, "Low frequency oscillations in a stationary plasma thruster," J. Appl. Phys. **84**, 3541 (1998).
[35]S. Mazouffre, "Laser-induced fluorescence diagnostics of the cross-field discharge of Hall thrusters," Plasma Sources Sci. Technol. **22**, 013001 (2013), and references herein.
[36]S. Mazouffre, G. Bourgeois, L. Garrigues, and E. Pawelec, "A comprehensive study on the atom flow in the cross-field discharge of a Hall thruster," J. Phys. D: Appl. Phys. **44**, 105203 (2011).
[37]J. Vaudolon and S. Mazouffre, "Indirect determination of the electric field in plasma discharges using laser-induced fluorescence spectroscopy," Phys. Plasmas **21**, 093505 (2014).
[38]S. Mazouffre, S. Tsikata, and J. Vaudolon, "Development and characterization of a wall-less Hall thruster," in *Proceedings 50th Joint-Propulsion Conference* (Cleveland, Ohio), AIAA Paper 2014–3513 (2014).
[39]D. Gawron, S. Mazouffre, N. Sadeghi, and A. Héron, "Influence of magnetic field and discharge voltage on the acceleration layer features in a Hall effect thruster," Plasma Sources Sci. Technol. **17**, 025001 (2008).